Frictional contact and cohesion laws for Casagrande's shear test on granular materials by 3D DEM – comparison with experiments

V. Richefeu, M.S. El Youssoufi, R. Peyroux & C.Bohatier
Laboratoire de Mécanique et de Génie Civil, UMR UM2-CNRS 5508, Université Montpellier 2, France

ABSTRACT: We investigate the macroscopic behavior of cohesive granular materials using a three-dimensional Discrete Element Method (DEM). We test the relevance of various interaction laws between grains. Two frictional contact laws and three different formulations of cohesion are used. The richest description is provided by a capillary cohesion model depending on the volume of liquid bonds. Using a spatial distribution of these volumes, we are able to study the case of wet granular media in the pendular state. The direct shear test is used for the simulations on cylindrical samples composed of spherical grains. Numerical results are compared to those of direct shear tests on glass beads. In both simulations and experiments, the water content is controlled. In particular, the comparison concerns shear strength and volume-changes. We show that simple contact laws and simple cohesion laws are sufficient to obtain a correct macroscopic behavior for the direct shear test.

1 INTRODUCTION

Discrete Element Methods (DEM) are based on the description of granular materials at the grain scale. Interactions between grains are modelled as laws which describe, more or less accurately, the physical phenomena at this scale.

In this work, the purpose is to study various interaction laws for the Casagrande's shear test on one hand, and to confront numerical results with experiments on the other hand. Experimental Casagrande's shear tests (Holtz & Kovacs 1991) have been realized on glass beads. Simulations are achieved in the same conditions as the experiments. They are meant to recover the observed macroscopic behaviors by using realistic parameters in the interaction laws.

2 DIRECT SHEAR TEST

2.1 *Principle of the test*

The sample is submitted to a compression force N normal to the shear plan (Figure 1). The lower part of the box is then translated at a constant velocity V_{shear} (The shear displacement is noted $\delta\ell$). During the test, we measure the shear force T and the sample height variation Δh. The mean shear strength is given by $\tau = T/S$, and the mean normal stress is given by $\sigma = N/S$, S being the sample section.

A set of tests with different normal stress allows us to evaluate the parameters of the shear strength envelope given by the Mohr-Coulomb linear law:

$$\tau = \tan(\varphi)\sigma + C \tag{1}$$

where C is the macroscopic cohesion and φ is the internal angle of friction.

2.2 *Numerical and experimental tests procedures*

We developped a three-dimensional code based on the classical Discrete Element Method (Cundall & Strack 1979).

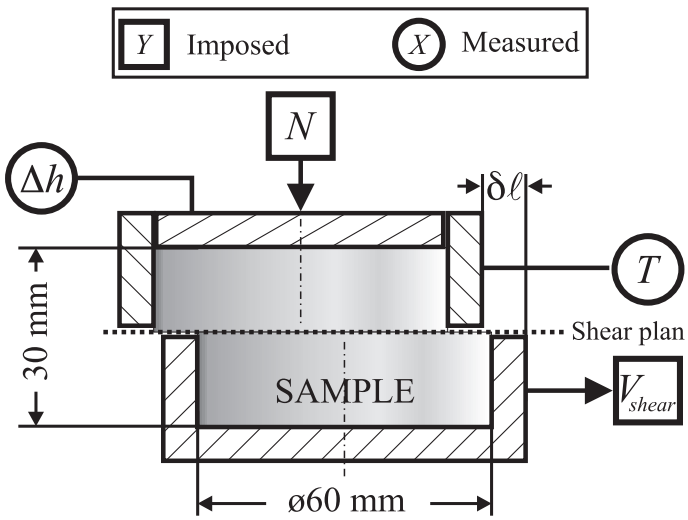

Figure 1. Illustration of the direct shear test and geometry of Casagrande's box.

In both numerical and experimental tests we use about 3600 glass beads of 3.0 ± 0.1 mm diameter. The glass beads density is 2546 kg.m^{-3}. Experimental samples are builted with solid fraction $c = 0,60 \pm 0,01$. Four numerical samples with solid fractions equal to 0.590, 0.595, 0.600 and 0.605 are obtained using a procedure of compaction by altering the inter-grains friction. The cohesion force between grains is assumed to result from water bonds. The equivalent water volume in the "wet" numerical samples is 3 ml. The time step is 10^{-6} s for all simulations.

3 INTERACTION MODELS

3.1 *Normal contact laws*

The normal repulsive contact force is usually splited into an elastic force F_n^{el} and a damping force F_n^{dis}. This force acts only if the inter-grain distance D_n is negative. We use two contact laws.

In the first contact law (Hertz), denoted by CTC1, the elastic force is given by:

$$F_n^{el} = \frac{4}{3}\left(\frac{1-\nu_1^2}{Y_1} + \frac{1-\nu_2^2}{Y_2}\right)^{-1} \sqrt{R_{eff}}(-D_n)^{\frac{3}{2}} \quad (2)$$

where $R_{eff} = R_1 R_2/(R_1 + R_2)$ is the effective radius of the interacting beads, Y_1 and Y_2 are their Young's moduli, and ν_1 and ν_2 are their Poisson's coefficients.

In the second contact law, denoted by CTC2, the elastic force is simply modelled as a linear spring:

$$F_n^{el} = -K_n D_n \quad (3)$$

The normal damping force is modelled, in both cases, as a dashpot that dissipates the kinetic energy of the bodies.

3.2 *Normal cohesion laws*

When a normal cohesion is taken into account, we add a negative term F_{coh} to the normal force. In the presence of the contact ($D_n < 0$), the cohesion force is set to a constant value: $F_{coh}(D_n = 0)$. We consider three different cohesion laws.

The first law, denoted by COH1, refers to the cohesion due to water bonds between grains. The capillary force is estimated by considering the liquid surface tension and the difference of pressure between liquid and gaz phases (Pierrat & Caram 1997; Mikami et al. 1998; Soulié et al. 2005). We use the capillary law proposed by Soulié et al. (see this volume). The cohesion force is given by:

$$F_{coh} = -\pi\gamma\sqrt{R_1 R_2}\,(\exp(AD_n^\star + B) + C) \quad (4)$$

where R_1 and R_2 are respectively the smaller and the bigger radiis, $D_n^\star = D_n/R_2$ is the dimensionless inter-grains distance, γ is the water surface tension, and A, B and C are parameters which depend on the liquid bond volume and the radius R_2.

The cohesion force acts on the interacting grains as long as a liquid bond exists. This is determined by a rupture distance criterion and a formation distance criterion both depending on the water distribution.

In the second law, denoted by COH2, the distribution of liquid bonds is not taken into account. The normal cohesion force depends only on D_n as follows:

$$F_{coh} = (F_{coh}^\circ/D^\circ)D_n - F_{coh}^\circ \quad (5)$$

where F_{coh}° is a constant positive value, and D° is a constant distance of rupture/formation.

The third law, denoted by COH3, is simply given by:

$$F_{coh} = -F_{coh}^\circ \quad (6)$$

In the two previous laws, the existence of the liquid bond is determined by the rupture/formation distance D°.

3.3 *Friction law*

The tangential friction force F_π is governed by the Coulomb law. The direction is opposite to the sliding velocity $\vec{V}_\pi^{rel}$. This friction force reads as follows:

$$\vec{F}_\pi = -\min(K_t||\vec{V}_\pi^{rel}||, \mu(F_n - F_{coh}))\frac{\vec{V}_\pi^{rel}}{||\vec{V}_\pi^{rel}||} \quad (7)$$

where K_t is the tangential stiffness.

4 NUMERICAL RESULTS

Numerical shear tests were performed using the two contact laws and the three cohesion laws. The corresponding parameters are given in Table 1.

Table 1. Material parameters for the interaction laws.

	Y (GPa)	ν (-)	
Grains	62	0.25	
Walls	200	0.3	
	μ (-)	K_n (N/m)	K_t (Ns/m)
Grain/grain	0.3	10^6	0.6 10^6
Grain/wall	0.15	10^6	0.6 10^6

We chose realistic values of Young's moduli and of Poisson's ratios for the law CTC1. The friction coefficients were measured. To estimate the constant force F_{coh}° and the constant distance D° for the laws COH2 and COH3, we first made a simulation with the law COH1 using realistic parameters. Then, we chose respectively the average values of the cohesion force and the rupture distance over a few time steps.

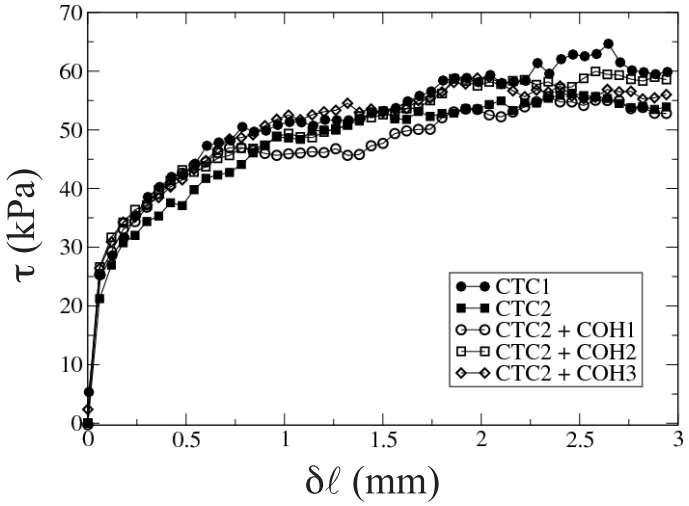

Figure 2. Shear strength τ as a function of shear displacement $\delta\ell$ with the different laws (σ = 120 kPa, c = 0.6).

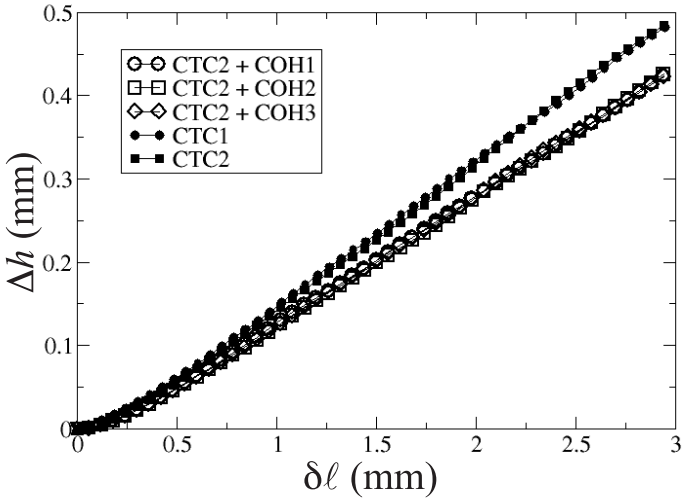

Figure 3. Sample height variation Δh as a function of shear displacement $\delta\ell$ with the different laws (σ = 120 kPa, c = 0.6).

The influence of the interaction laws on the macroscopic results can be seen in Figures 2 and 3. Interestingly, no marked effects of the local cohesion on the shear strength is observed. The height variation plots show that for the same shear displacement the volume change is larger in the dry case than in the wet case. The volume change is limited in the wet case by the cohesive actions between grains. Nevertheless, we can notice that the dry curves, on the one hand, and the wet curves, on the orther hand, can not be distinguished.

Figure 4 shows, for each law, the evolution of the major principal direction of the fabric tensor (inclination α to the horizontal). For all laws, this direction is initialy 80˚: this situation is due to the only action of the normal force N. As soon as the shear test begins, the inclination angle decreases drastically to reach the value of about 40˚.

In summary, local cohesion influences slightly the volume change during the shear test. Indeed, with quasistatic loading and confined sample, contact forces are much larger than the capillary cohesion forces. In the simulations, the mean compressive

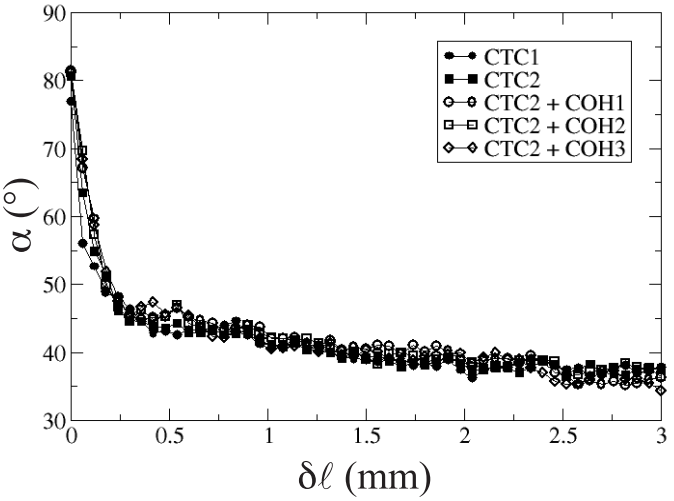

Figure 4. Major principal direction α of the fabric tensor for the different laws.

force is about 1 N for the entire contact network and about 5 N for the strong network. Comparatively, the largest capillary force is only about 4.10^{-3} N. The macroscopic stress-strain behavior is thus practically not affected by the local cohesion. For a better comparisons of the cohesion laws, we should carry out tests with larger number of grains, polydisperse materials or other test configuration. Concerning the contact laws, macroscopic results do not show significant differences between the two laws. So, in order to reduce the computation cost, it seems useful to take into account the simplest law ; i.e. the linear one.

5 EXPERIMENT/SIMULATION COMPARISON

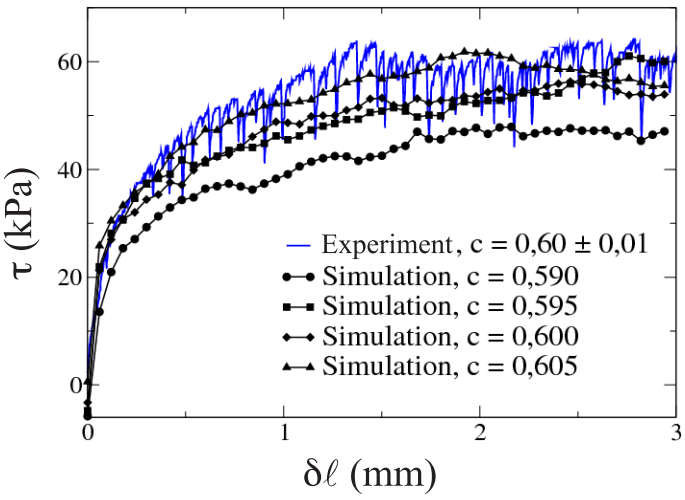

Figure 5. Shear strength for different initial values of the solid fraction (σ = 120 kPa). The experimental result is shown.

In order to confront the results of simulations with experiments, we carried out shear tests with the CTC2 law. Experimental tests on dry glass beads were also performed.

Simulations are carried out in the same conditions as the experiments (sample, boundary conditions and loading).

The numerical and experimental results of shear strength are in good qualitative and quantitative agreement ; Figure 5. In particular, the best estimation is obtained with a solid fraction of 0.605.

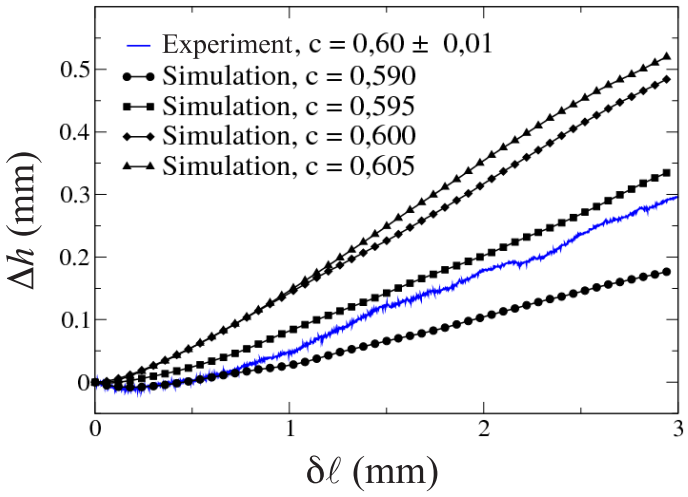

Figure 6. Sample height variation for different initial values of the solid fraction (σ = 120 kPa). The experimental result is shown.

Computed height variations agree qualitatively with the experimental results ; Figure 6. The initial value of the solid fraction is a major state parameter that determines the volume changes of the sample. Actually, a slight variation of the initial value of solid fraction can strongly modify the material behavior.

6 CONCLUSION

Results of 3D simulations of Casagrande shear tests have been presented. We studied the relevance of different interaction laws in this case. In our simulation conditions, the contact laws were found to be equivalent. This implies that a gain in computation time can be obtained by using a simple linear contact law without significant impact on the macroscopic results and on the texture of the granular material. The dominant action of the contact forces, due to the quasistatic and confined feature of the test, masks the influence of the capillary cohesion on the shear strenght. The only effect of local cohesion, in our simulations, concerns the volume-change behavior. Other simulations with more grains, polydisperse materials and/or different loadings should be performed to obtain a better comparison between the cohesion laws.

The simplest contact law was used to confront the numerical results with the experimental ones. A good qualitative and quantitative estimation of the macroscopic results was obtained. We clearly observe the dominant effect of the initial value of solid fraction on the volume-change behavior.

References

Cundall, P. & Strack, O. 1979. A discrete numerical model for granular assemblies. *Géotechnique 29*(1): 47–65.

Holtz, R. & Kovacs, W. 1991. *Introduction à la Géotechnique*. Edition de l'École Polytechnique de Montréal.

Mikami, T., Kamiya, H., & Horio, M. 1998. Numerical simulation of cohesive powder behavior in fluidized bed. *Chemical Engineering Science 53*(10): 1927–1940.

Pierrat, P. & Caram, H. 1997. Tensile strength of wet granular materials. *Powder Technology* 91: 83–93.

Soulié, F., El Youssoufi, M. S., Cherblanc, F., & Saix, C. 2005. Influence of water content on the mechanical behavior of granular assemblies. In *Powders and grains (this proceeding)*. A.A. Balkema.